Iraqi Journal of Science
ISSN: 0067-2904

Fabrication and Enhancement UV Photodiode Based on Mg-Doped ZnO Nanorods Films

Hussein Abdullah Hameed*[1], J. J. Hassan[2], H. L. Saadon[2]
[1] Department of Physics, College of Science, Kufa Uniersity, Najaf, Iraq
[2] Department of Physics, College of Science, Basrah Uniersity, Basrah, Iraq

Abstract

Magnesium-doped Zinc oxide (ZnO: Mg) nanorods (NRs) films and pure Zinc oxide deposited on the p-silicon substrates were prepared by hydrothermal method. The doping level of the Mg concentration (atoms ratio of Mg to Zn was chosen to be 0.75% and 1.5%. X-ray diffraction (XRD) and energy-dispersive X-ray spectroscopy (EDX) were performed to characterize the prepared films. X-ray diffraction analysis showed a decrease in the lattice parameters of the Mg-doped ZnO NRs. Under 10V applied bias voltage, the responsivity of p-n junction UV photodiode based on pure ZnO and Mg: ZnO with doping ratio (0.75% and 1.5%) was 0.06 A/W and (0.15A/W and 0.27A/W) at UV illumination of wavelength 365 nm respectively, 0.071 A/W and (0.084A/W and 0.11A/W) for UV wavelength of 385 nm with power density 40µW/cm2, respectively. The Mg-doped ZnO NRs photodiode exhibited high photosensitivity, fast response and fall times, and good orientation properties.

Keywords: pure ZnO, nanorod, Mg doping ZnO, photodiode, hydrothermal method.

تصنيع وتحسين كواشف الاشعة فوق البنفسجية المعتمدة على القضبان النانوية للزنك اوكساید النقي والمشوب بالمغنيسيوم

حسين عبدالله حميد[1]*، جلال جبار حسن [2]، هيثم لفته سعدون [3]
[1]قسم الفيزياء، كلية العلوم، جامعة الكوفة، النجف، العراق
[2] قسم الفيزياء، كلية العلوم، جامعة البصرة البصرة، البصرة، العراق

الخلاصة

تم تحضير اغشية أوكسيد الزنك النقية المشوبة بالمغنيسيوم بتراكيز مختلفة على قواعد سيليكون نوع p بالطريقة الحرارية المائية . اخذت نسب ذرات المغنيسيوم الى الزنك كمستوى للتشويب بحدود 0% 0.75% 1.5% . تم اجراء فحوصات حيود الأشعة السينية ((EDX،XRD)) لتوصيف الاغشية المحضرة وتحديد نسب التشويب عمليا. أظهرت تحليلات حيود الأشعة السينية(XRD) بان جميع النماذج متعددة البلورات ذات تركيب سداسي بالاتجاه (002). عند تحيز الكاشف عند 10 V ، كانت الاستجابية للزنك اوكساید والمشوب بالمغنيسيوم بتراكيز 0% ,0.75% ,1.5% تحت اشعة الفوق البنفسجية ذات شدة 40 µ واط / سم 2 عند طول موجي 365 نانومتر 0.06 A/W ,0.15A/W ,0.27A/W على التوالي. وكانت الاستجابة عند طول موجي 385 نانومتر 0.071 A/W , 0.084A/W , 0.11A/W. كما تم حساب الاكفاءة والكشفية والمعاملات الاخرى للكواشف اعلاه لعدت فولتيات ولمدى من الاطوال الموجية.

*Email: husseina.alshemirti@uokufa.edu.iq

Introduction

Zinc oxide(ZnO) is a semiconductor material composed of zinc ions Zn^{2+} and oxygen ions, . It has special optical and electrical properties. It has a large energy gap and a relatively large exciton binding energy of about 3.37eV and 60 MeV, respectively at room temperature[1]. There are several reports focused on efforts to control the properties of ZnO by adding transition metal impurities such as Al[2], Cu[3] or In[4]. Doping to control and adjust the band gap, greatly contributes to increase the efficiency and power in many applications, such as Light-emitting diodes[5], laser diodes[6], solar cells, transparent electrodes, thin film transistors and optical sensors [7, 8]. The ZnO sensing mechanism is highly correlated with surface reactions hence; oxygen absorption, grain size, defects, and other parameters have an important effect in controlling the sensing response. In the present study, systematic Mg doping (0, 0.75%, and 1.5%) in ZnO NPs was achieved and analyzed by XRD, EDX. The performance of p-n junction photodiode fabricated using Mg-doped ZnO that produce the highest responsivity, quantum efficiency and others parameters compared with a pure ZnOwas discussed..

Experimental

The hydrothermal method was used to synthesize a pure and Mg-doped ZnO as reported by several researchers [7, 9]. First,many stages of ultrasonic cleaning was to clean the p-Si substrate , starting with ethanol, acetone, and propanol for 10 minutes with each solvent, then it was cleaned with deionized water and dried. Zinc acetate dehydrates 0.05 M was first dissolved in ethanol with stirring at 60c° for (2-3) hours until a clear and transparent homogeneous solution was formed. A homogeneous seed layer was obtained by a spin coating technique, wherethe prepared solution was poured over the center of a substrate using a dropper, at a rate of

2000 for 30 seconds. This process was repeated several times on hotpot temperatures 0f about (140-150) c° for 10 min per cycle to remove the solvent, Finally, the samples were annealed at (350-400) c° in a furnace for 2 h to obtain the ZnO seed layer. After the formation of a seed layer, ZnO nanorods were formed through the hydrothermal method. The substrates with a seed layer of ZnO were placed verticality inside Teflon vessels filled with aqueous solution of 0.05M Zinc nitrate hexahydrate $Zn(NO_3)_2.6H_2O$ and 0.05 M Hexamethylenetetramine $C_6H_{12}N_4$, sealed and heated at (110-120) c° for 3 h. Then, the substrate was removed from the Teflon vessel, cleaned with distilled H_2O and dried. Next, the Mg-doped ZnO samples were grown on the seed-layer-coated Si substrate using aqueous solutions of 0.05M zinc nitrate hexahydrate, 0.05M Hexamethylenetetramine and at concentrations (the atoms ratio Mg to Zn atoms)of Mg/Zn (0.75%, 1.5%) magnesium nitrate $Mg(NO_3)_2.6H_2O$ as illustrated in Table1. These reagents were dissolved and reacted in Teflon vessel with a temperature of (110-120) c◦ for 3h. The substrate was rinsed with distilled water and all the samples were annealed for 2h in furnace at 350C◦. Then aluminium contacts were deposited on the upper films and on the bottom of the Si substrate (see Figure-1) by the thermal evaporator technique to produce p-n junction photodiode.

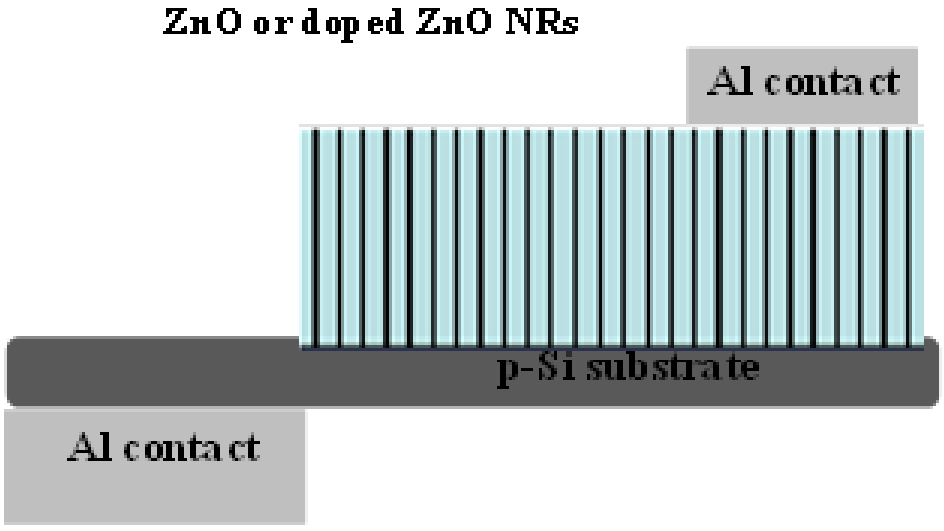

Figure 1- Schematic p-n junction photodiode based on pure and doped ZnO nanorods, Al deposited onto p-Si substrate

Table 1- The samples used in this work.

samples	element	ratio atoms Mg/ atoms Zn doped ZnO
S1	pure ZnO	0
S6	Mg	0.75%
S7	Mg	1.5%

Results and discussions

X-Ray Diffraction pattern

XRD patterns of ZnO and Mg: ZnO of doping ratio (1.5%) deposited on the p-type silicon substrate are show in Figure-2. For the pure ZnO, the diffraction peaks are at positions 31.8754, 34.238, 36.02, 47.37, 56.35 and 62.78 which correspond to the orientations (1 0 0), (0 0 2), (1 0 1), (1 0 2), (1 1 0) and (1 0 3), respectively.

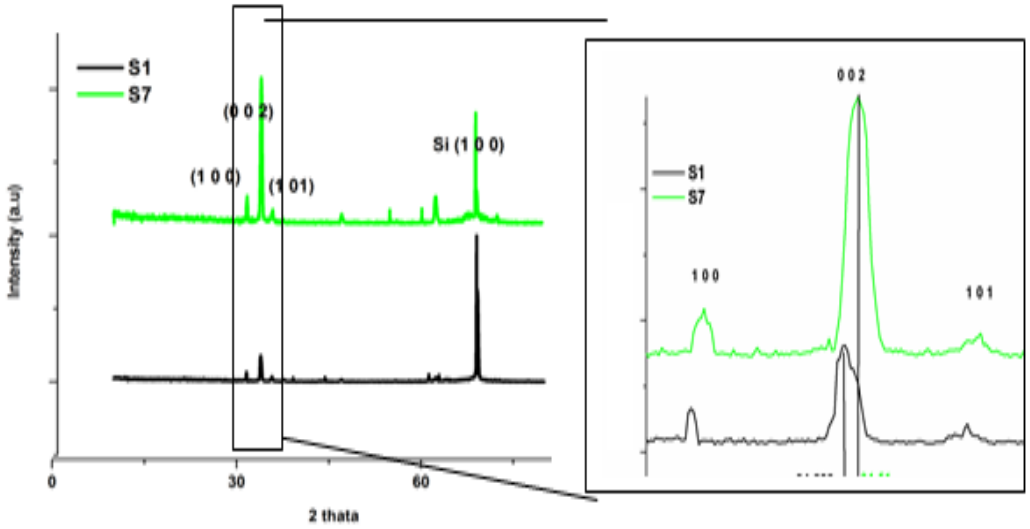

Figure 2- XRD patterns for undoped ZnO and Mg-doped ZnO for sample S7 (1.5%) deposited on the Silicon substrate

The position of the peaks well fit with a hexagonal wurtzite-type structure of ZnO. A strong peak at 2θ= 68.78 is due to the diffraction peak of silicon substrate. it can also be noticed that the diffraction peak at (0 0 2) has high intensity. This indicates that ZnO nanorods are vertically aligned on the Si substrate. While the diffraction peaks of Mg-doped ZnO for sample S7 (1.5%) were shifted towards higher angle due to the doping with Mg , due to the substitution of Zn^{+2} ions by Mg+ ions in the hexagonal lattice. No new phases were observed, this means that the doping with Mg not change the structure of ZnO. The mathematical equations of interplanar spacing, lattice constants a, c [10, 11], and the micro-strain [12] were calculated and shown in Table-2.

Table 2- Structural properties of the pure ZnO and ZnO doped Mg deposited on the Si substrate

names	h k l	2 θ °	FWHM 2 θ °	d (A°)	a (A°)	c (A°)	ε	c/a
S1	1 0 0	31.8754	0.303	2.80555	3.23957	5.23431	0.07284	1.61574
	0 0 2	34.238	0.469	2.61716			0.11206	
	1 0 1	36.02	0.351	2.48499			0.08343	
S7	1 0 0	31.9505	0.352	2.79912	3.23215	5.1943	0.0846	1.60707
	0 0 2	34.51	0.292	2.59715			0.06972	
	1 0 1	36.2	0.334	2.47968			0.07937	

EDX Analysis

EDX analysis of the undoped and Mg-doped ZnO nanorods for samples S1 (ZnO), S2 (0.75%) and S3 (1.5%) deposited on the silicon substrate are shown in Figure-3 and Figure-4 respectively. These results revealed the presence of Zn, O, Mg and Si elements where Si peaks originating from the substrate.

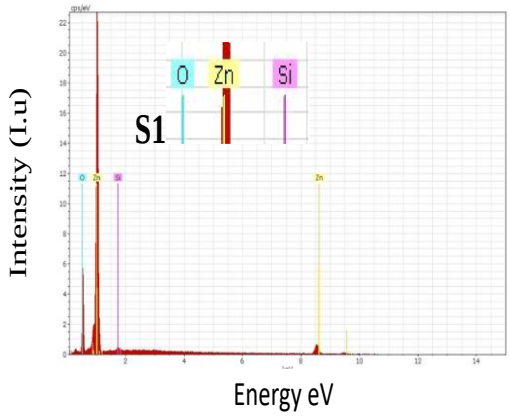

Spectrum: Acquisition

Element	Series	norm. C [wt.%]	Atom. C [at.%]
Oxygen	K-series	22.50	54.05
Silicon	K-series	0.50	0.69
Zinc	L-series	77.00	45.26
	Total:	100.00	100.00

Figure 3- EDX spectrum for ZnO deposited on the silicon substrate

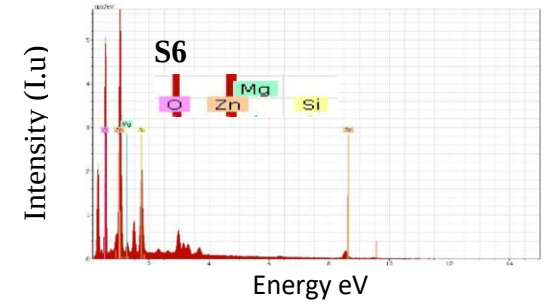

Spectrum: Acquisition

Element	Series	norm. C [wt.%]	Atom. C [at.%]
Oxygen	K-series	40.96	68.84
Silicon	K-series	10.91	10.45
Zinc	L-series	46.80	19.25
Magnesium	K-series	1.33	1.47
	Total:	100.00	100.00

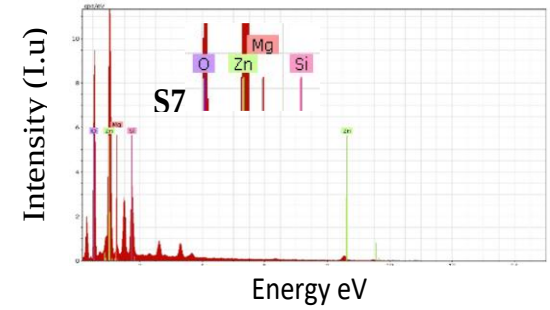

Spectrum: Acquisition

Element	Series	norm. C [wt.%]	Atom. C [at.%]
Oxygen	K-series	40.04	68.36
Silicon	K-series	9.79	9.52
Zinc	L-series	48.52	20.26
Magnesium	K-series	1.65	1.86
	Total:	100.00	100.00

Figure 4- EDX spectrum of Mg-doped ZnO for samples S6 (0.75%) and S7 (1.5%) deposited on the Silicon
Substrate

Characteristics Measurement of the HJ UV Photodiodes

All HJ photodiodes were measured in dark and under UV of wavelengths 365 nm and 385 nm of a power density 40 μW/ cm^2 They were studied under variable reverse bias voltages of 0.5, 1, 3, 5, 10, and 15 V at room temperature. The active area of these photodiodes was about 0.5 cm^2 ±0.05cm^2.

J-V Characteristics and Responsivity

J-V characteristics of the HJ ZnO/p-Si photodiodes were measured at room temperature, in dark and under the UV of wavelengths 365nm and 385 nm as shown in Figure-5. For sample , for S1(ZnO), the results of the current density and responsivity under UV of 385 nm wavelength were greater than the current density and responsivity for UV 365 nm wavelength. The reason may be because the cut-off at the wavelength of 385nm is nearly close to the Zinc oxide energy gap of 3.27eV and the decrease of penetrating depth of the light at the shorter 365nm wavelength.

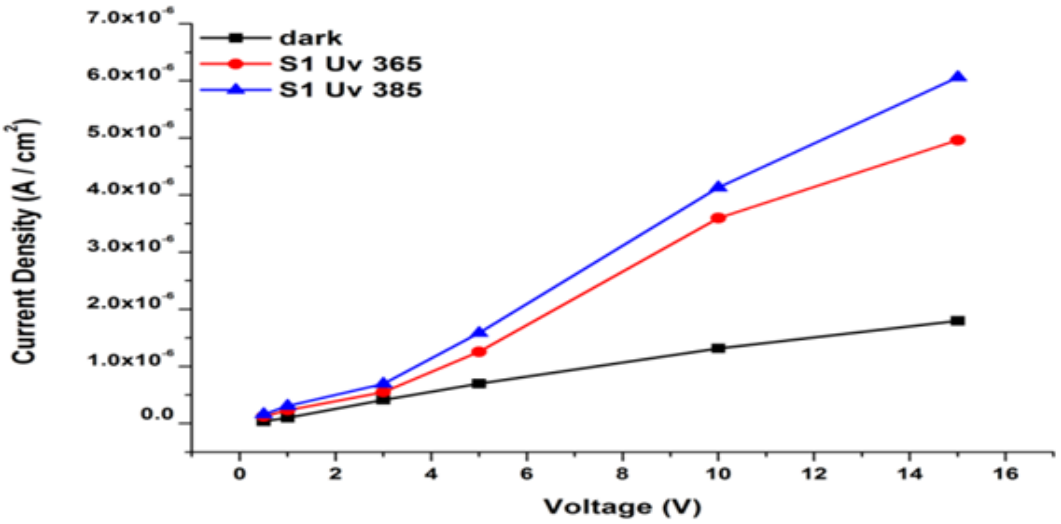

Figure 5- J–V characteristics of the HJ ZnO photodiode in dark and under illumination of UV wavelengths
365nm and 385nm

From the above figure, it is possible to determine the optimum range of bias voltage , that gives the best responsivity at wavelengths 365 nm and 385 nm. In addition, J-V curves of the HJ Mg- doped ZnO/p-Si photodetectors , samples S6 (0.75%) and S7 (1.5%) , in the dark and under UV of wavelengths 365 nm and 385 nm were measured as shown in Figure -6a and Figure -6b, respectively.

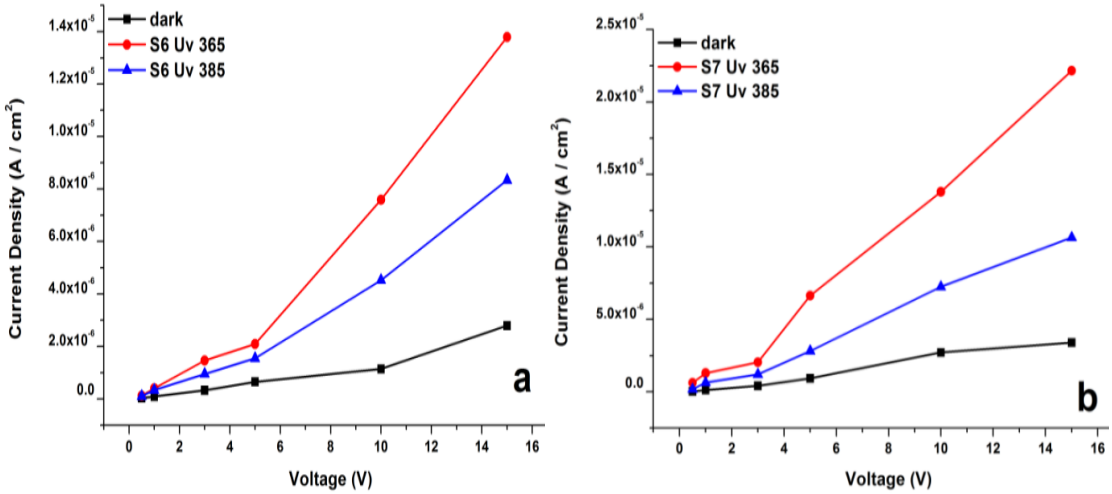

Figure 6- J–V characteristics of the HJ Mg-doped ZnO photodiode in dark and under illumination of UV wavelengths 365nm and 385nm for samples a) S6 (0.75%) b) S7 (1.5%)

The responsivities of HJ ZnO/p-Si and Mg-doped ZnO/p-Si photodiode under UV illumination of 365 nm and 385 nm wavelengths at room temperature are shown Figure-7a and Figure-7b respectively. Responsivities of the samples S6 and S7 under UV illumination of wavelength 365 nm were 0.15A/W,0.27A/W respectively, while for UV illumination of wavelength 385 nm were 0.084A/W and 0.11A/W respectively. The values of the photosensitivity[13], quantum efficiency [14] gain [15] and specific detectivity (D) [16] at a wavelength of 365 and 385 nm are shown in Table-3.

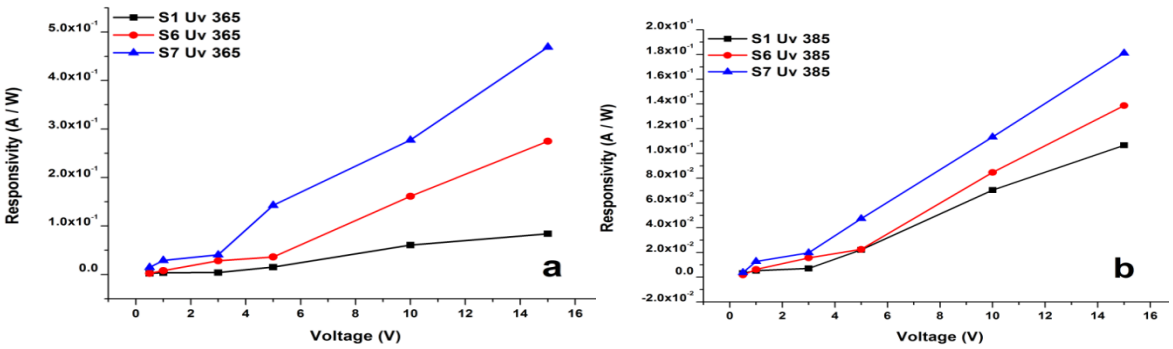

Figure 7- Responsivity as a function of voltage for the HJ photodiodes based on Mg-doped ZnO and ZnO under a) UV 365 light b) UV 385 light

Table 1- parameters of the HJ photodiodes for ZnO and Mg-doped ZnO as a function of voltage at wavelengths
365nm and 385 nm

parameters	voltage	365 nm			385 nm		
		S1	S6	S7	S1	S6	S7
quantum efficiency %	0.5	0.00726	0.00784	0.05018	0.01006	0.00582	0.012
	1	0.0114	0.02676	0.099	0.01673	0.0201	0.04113
	3	0.01166	0.09652	0.13807	0.02255	0.0504	0.0637
	5	0.04737	0.12277	0.48519	0.07131	0.07243	0.15264
	10	0.19398	0.54817	0.94272	0.22711	0.27288	0.36543
	15	0.26906	0.93508	1.59539	0.34382	0.44734	0.58415
Photosensitivity %	0.5	224.98013	279.46128	1932.7466	328.67834	218.85522	4.87616
	1	132.54246	341.47077	943.18113	205.07626	270.58469	4.13365
	3	33.10667	347.02961	390.06665	67.5408	191.11228	1.89819
	5	79.64479	221.75867	616.9563	126.46684	138.00017	2.04732
	10	173.2959	565.58092	409.09219	214.00446	296.97246	1.67269
	15	175.96544	393.96153	552.77774	237.18023	198.79808	2.13489
specific detectivity	0.5	4.7302E10	5.2231E10	3.4750E11	6.5889E10	4.0905E10	8.7672E10
	1	6.4348E10	1.5084E11	4.8221E11	9.4929E10	1.1952E11	2.1134E11
	3	5.6322E10	5.0025E11	6.3431E11	1.0955E11	2.7549E11	3.0867E11
	5	2.2731E11	5.8222E11	1.9306E12	3.4415E11	3.6232E11	6.4066E11
	10	9.5962E11	2.7786E12	3.0990E12	1.1299E12	1.459E12	1.2671E12
	15	1.3947E12	3.7095E12	5.7396E12	1.7925E12	1.87191E12	2.21671E12
Gain	0.5	3.2498	3.79461	20.32747	4.28678	3.18855	5.87616
	1	2.32542	4.41471	10.43181	3.05076	3.70585	5.13365
	3	1.33107	4.4703	4.90067	1.67541	2.91112	2.89819
	5	1.79645	3.21759	7.16956	2.26467	2.38	3.04732
	10	2.73296	6.65581	5.09092	3.14004	3.96972	2.67269
	15	2.75965	4.93962	6.52778	3.3718	2.98798	3.13489

The Photoswitching Characteristics

Figure-8 shows the photoswitching characteristics of the undoped Zinc oxide thin film based photodiode under UV illumination of wavelengths 365 nm and 385 nm, with 10 V bias voltage. The oxygen molecules play an important role in the response process when ultraviolet radiation is applied to the detector, the photocurrent returns to a primitive value in the absence of ultraviolet light (as in the case of darkness)[16].

The maximum photocurrent density of the detector was 2.28μA/cm2 under illumination of UV of 365 nm. This is significantly smaller than when the detector is under illumination UV at 385 nm which was 2.7μA/ cm^2. While the photocurrent density of the samples S6 (0.75%) and S7 (1.5%) was 6.45 μA/ cm^2 and 11.21. μA/ cm^2 under illumination of UV wavelength 365 nm, respectively (see Figure-9a). It was about 3.3 μA/ cm^2 and 4.47 μA/ cm^2 for illumination of UV wavelength 385 (as shown in Figure-9b). These values were measured under the ON/OFF switching UV light with a time duration of 10 sec/10 sec respectively, under 10V applied bias voltage .

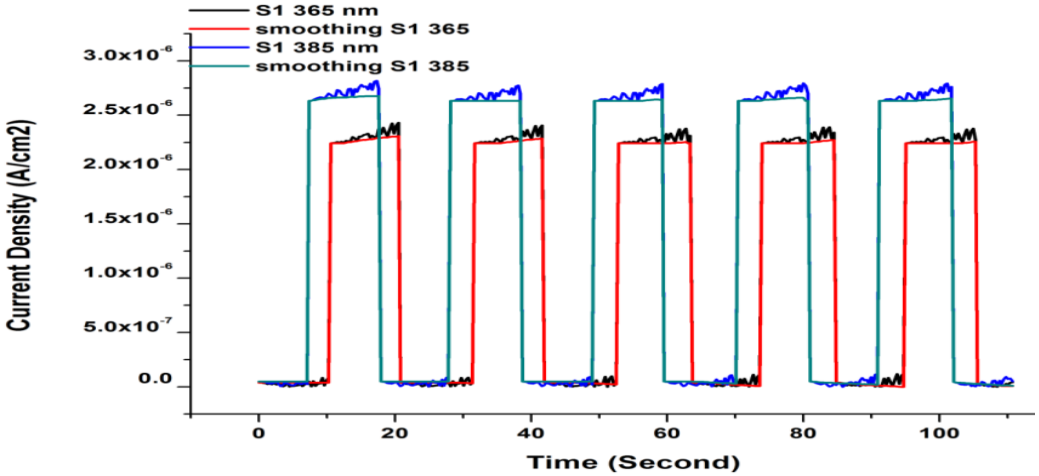

Figure 8- Current density -Time of the HJ ZnO photodiode under UV of wavelengths 365nm and 385 nm at 10V bias

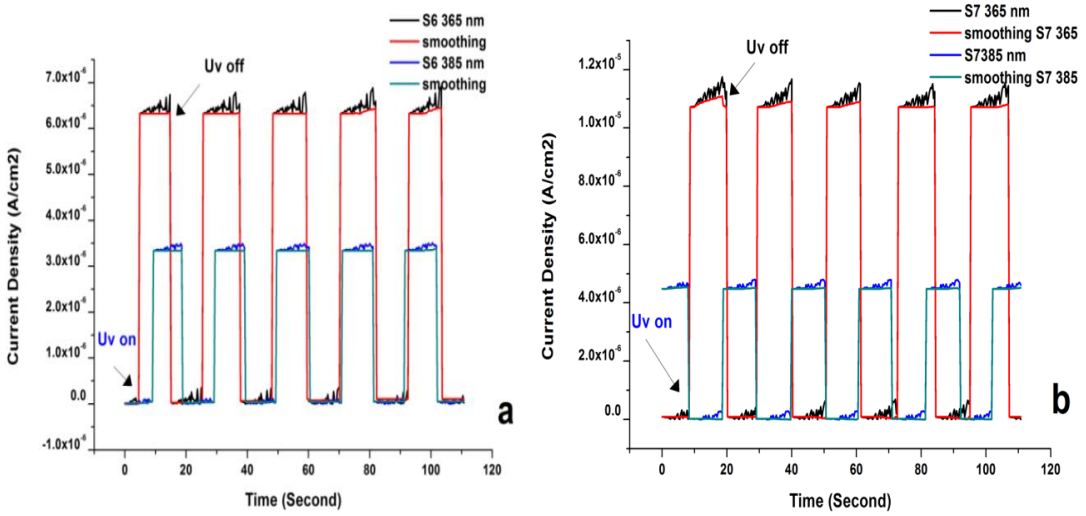

Figure 9- Current density -Time of the HJ ZnO photodiode under UV of wavelengths 365nm and 385 nm at 10V bias voltage.

The responsivity of the photodiodes was considered as the main parameter to be checked The UV (wavelengths 365 nm and 385 nm) detection stability switching (on and off) was recorded periodically at regular time intervals of 10 s as showed in Figure-10. The responsivity of samples S6 and S7 photodiodes were 0.156A/W and 0.0271 A/W under UV 365 nm respectively, 0.082 A/W and 0.11 A/W for UV 385 nm.

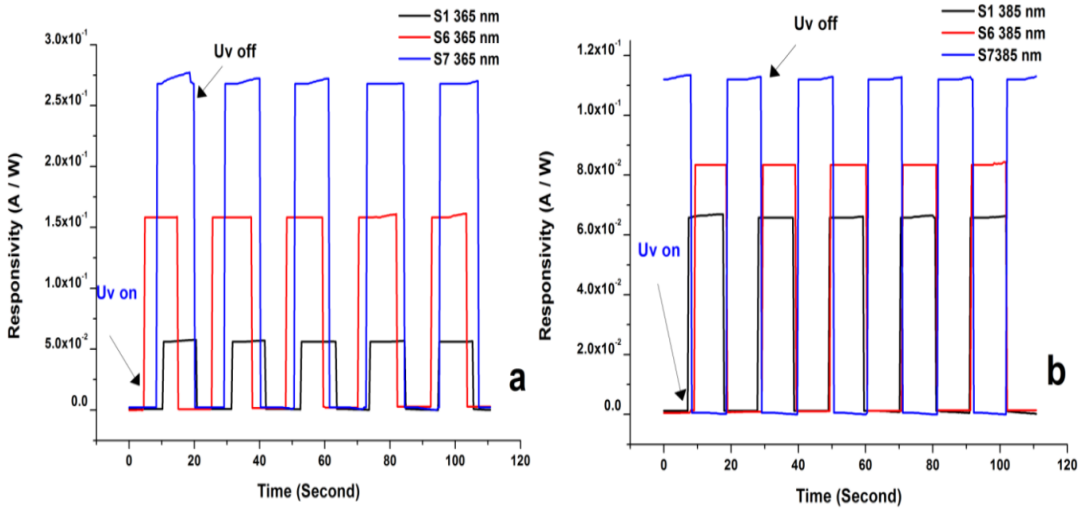

Figure 10- Responsivity with a time of the HJ photodiode based on Mg-doped ZnO (S6=1%) and (S7=1.5%) compared with photodiode based on ZnO under a) UV 365 nm b) UV 385 nm

The Mg-doped ZnO photodiodes can work as photovoltaics to detect ultraviolet rays with a high-speed response and recovery without an external source when exposed to ON/ OFF switch 365 nm and 385 nm of UV light, as shown in Figure-11. The maximum responsivity of the samples S6 and S7 were 6×10^{-4} and 2.3×10^{-3} A/W at UV wavelength of 365 nm, 2.1×10^{-4}, and 6.1×10^{-4} at wavelength 385 nm of UV, under 0 V applied bias voltage

.

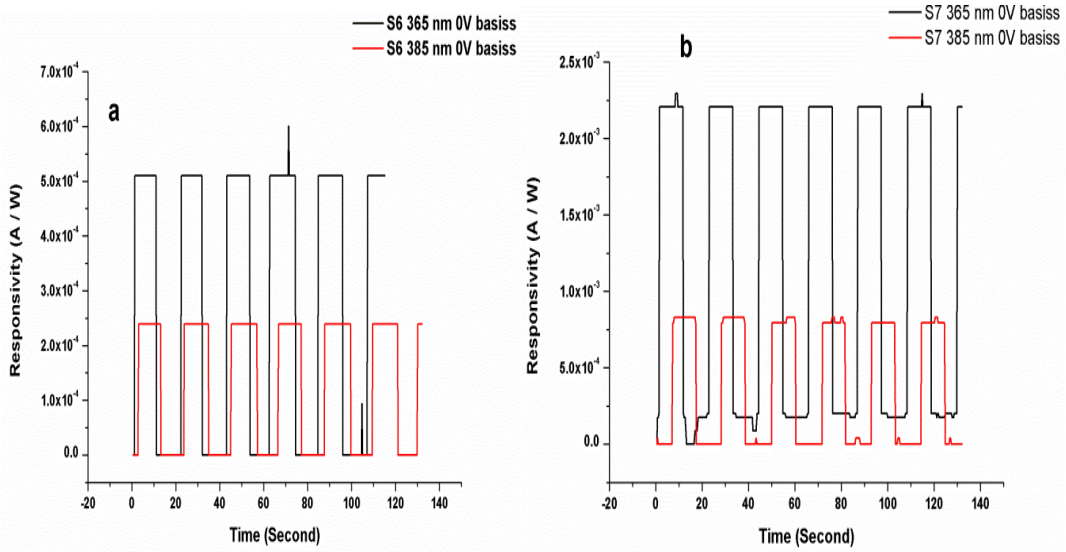

Figure 11- Responsivity -Time of the photovoltaic based on Mg-doped under UV 365nm and 385 nm at 0 V bias for samples a) S6 (0.75%) and b) S7 (1.5%)

Responsivity and Quantum Efficiency as a Function of Wavelength

All heterojunction photodiodes at room temperature under 1V applied reverse bias voltagewere studied using a Xenon lamp of wavelength 325 nm -550nm. The responsivity and quantum efficiency curves of HJ ZnO/p-Si photodiode and only Si substrate at room temperature are shown in Figure-12a and Figure-12b , respectively. The responsivity values and quantum efficiency increase with an increase in the wavelength up to 385 nm to reach about 0.0094A/W and 2.95% respectively. It decreases at higher wavelengths because the ZnO detector has poor performance in the visible region. But a gradual increase in response at longer wavelengths for all HJ photodiode was noticed and this is due to the silicon base of the detector, where silicon has a much lower energy gap than ZnO. These results indicate that all HJ photodiodes may be able to detect UV and visible light .

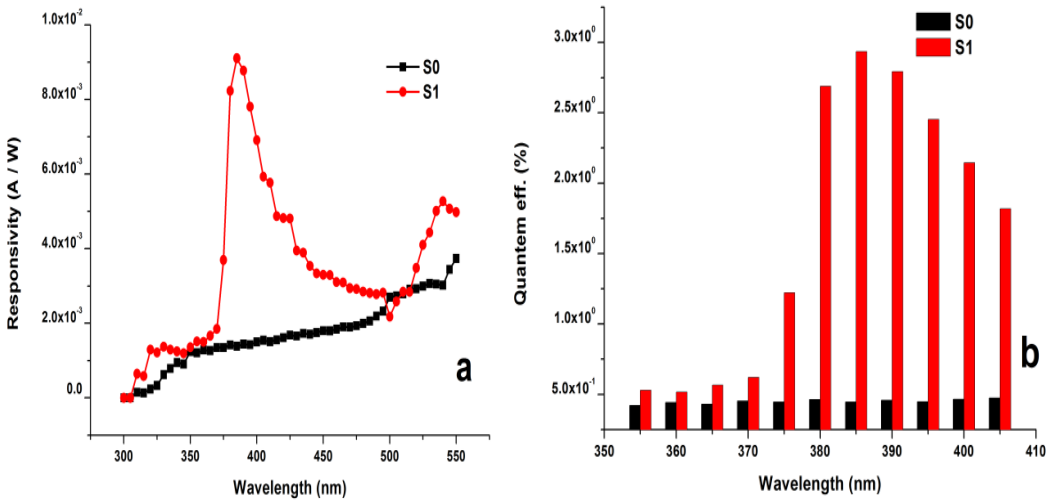

Figure 12- a) Responsivity and b) quantum efficiency as function wavelength for HJ ZnO photodiode and Si Substrate

In addition, the responsivity and quantum efficiency curves for Mg-doped ZnO Si photodiodes are shown in Figure-13a and Figure-13b, respectively. The responsivity spectrum of photodiodes shows a broadband in the wavelength region 360 to 400 nm with a maximum responsivity at about 380 nm.

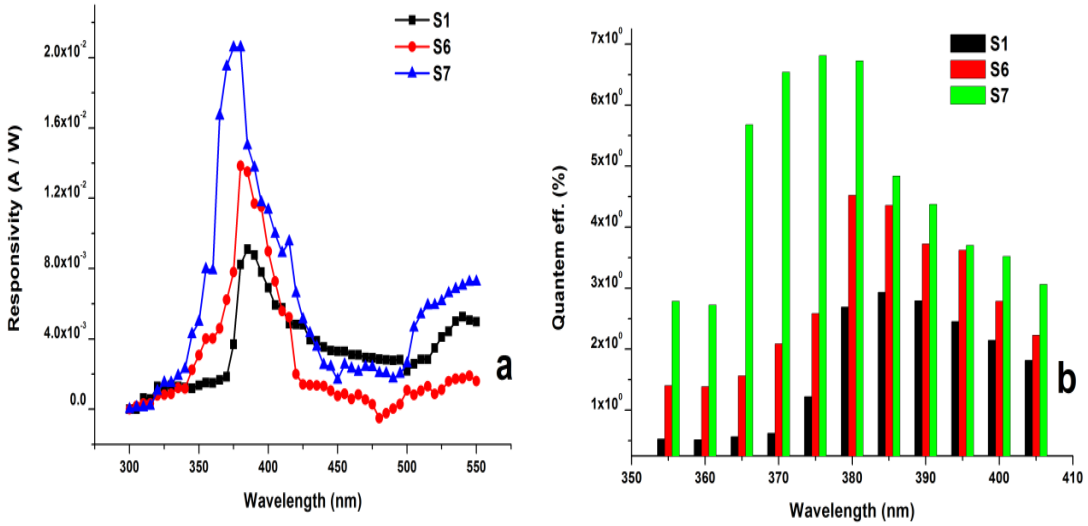

Figure 13- a) Responsivity and b) quantum efficiency as function wavelength for HJ ZnO photodiode and Si substrate

Conclusions

In this work, the structural, optical, electrical and compositional properties for pure and Mg-doped ZnO/p-Si, synthesized by the hydrothermal method, were studied. The UV photodiode has been fabricated on a base of pure and Mg-doped ZnO. The photoresponse properties under UV illumination at wavelengths 365nm and 385 nm were studied at room temperature. The performance of the photodiode can be improved with respect to the photocurrent, responsivity, photosensitivity, and specific detectivity. The UV photodiode based on an Mg-doped ZnO has shown enhanced responsivity and quantum efficiency in addition to the other parameters under an applied voltage of 10 V d.

References

1. Janotti, A. and C.G. Van de Walle. **2009**. *Fundamentals of zinc oxide as a semiconductor*. Reports on progress in physics. **72**(12): 126501.
2. Yun, S., et al. **2010**. Hydrothermal synthesis of Al-doped ZnO nanorod arrays on Si substrate. *Physica B: Condensed Matter*. **405**(1): 413-419.

3. Chow, L., et al. **2013**. Synthesis and characterization of Cu-doped ZnO one-dimensional structures for miniaturized sensor applications with faster response. *Sensors and Actuators A: Physical*. **189**: 399-408.

4. Guo, M., P. Diao, and S. Cai. **2005**. Hydrothermal growth of well-aligned ZnO nanorod arrays: Dependence of morphology and alignment ordering upon preparing conditions. *Journal of Solid State Chemistry*. **178**(6): 1864-1873.

5. Zhuang, Y.D., et al. **2013**. Fabrication and characterization of light-emitting diodes comprising highly ordered arrays of emissive InGaN/GaN nanorods. *IEEE Photonics Technology Letters.* **25**(11): 1047-1049.

6. Song, J. **2014**. *Fabrication and Characterization of Edge-Emitting Semiconductor Lasers*. Thesis (M.S.)--Rose Hulman Institute of Technology

7. Santoshkumar, B., et al. **2017**. *I*nfluence of defect luminescence and structural modification on the electrical properties of Magnesium Doped Zinc Oxide Nanorods. *Superlattices and Microstructures*. **106**: 58-66.

8. Lu, Y., I. Dajani, and R. Knize. **2006**. ZnO nanorod arrays as pn heterojunction ultraviolet photodetectors. *Electronics Letters*. **42**(22): 1309-1310.

9. Fu, M., et al., **2011**. Sol–gel preparation and enhanced photocatalytic performance of Cu-doped ZnO nanoparticles. *Applied Surface Science*. **258**(4): 1587-1591.

10. Feng, Z.C. **2012**. *Handbook of zinc oxide and related materials: volume two, devices and nano-engineering*. Vol. 2: CRC press.

11. Iqbal, A., M. Zakria, and A. Mahmood. **2015**. Structural and spectroscopic analysis of wurtzite (ZnO) 1− x (Sb2O3) x composite semiconductor. *Progress in Natural Science: Materials International*. **25**(2): 131-136.

12. Bindu, P. and S. Thomas. **2014**. Estimation of lattice strain in ZnO nanoparticles: X-ray peak profile analysis. *Journal of Theoretical and Applied Physics*. **8**(4): 123-134.

13. Al-Salman, H.S. and M. Abdullah. **2015**. Annealing Effects on the Structural, Optical, and UV Photoresponse Properties of ZnO Nanostructures Prepared by RF-Magnetron Sputtering at Different Deposition Temperatures. *Acta Metallurgica Sinica* (English Letters). **28**(2): 230-242.

14. Deen, M.J. and P.K. Basu. **2012**. *Silicon Photonics: Fundamentals and Devices*. Vol. 44: John Wiley & Sons.

15. Joshi, N. **2017**. *Photoconductivity: art: science & technology*: Routledge.

16. Li, S.S. **2012**. *Semiconductor physical electronics*: Springer Science & Business Media.